Biochemical and Biophysical Research Communications 421 (2012) 232–238

Contents lists available at SciVerse ScienceDirect

Biochemical and Biophysical Research Communications

journal homepage: www.elsevier.com/locate/ybbrc

Splicing transitions of the anchoring protein ENH during striated muscle development

Jumpei Ito [a], Taiki Hashimoto [a], Sho Nakamura [a], Yusuke Aita [b], Tomoko Yamazaki [b], Werner Schlegel [c], Koichi Takimoto [a], Andrés D. Maturana [a,b,*]

[a] Department of Bioengineering, Nagaoka University of Technology, 1603-1 Kamitomioka, Nagaoka, Niigata 940-2188, Japan
[b] Global Edge Institute, Tokyo Institute of Technology, Tokyo 152-8550, Japan
[c] Fondation pour Recherches Médicales, Medical Faculty, University of Geneva, Geneva 1211, Switzerland

ARTICLE INFO

Article history:
Received 22 March 2012
Available online 4 April 2012

Keywords:
Scaffolding protein
Alternative splicing
C2C12
Heart

ABSTRACT

The ENH (PDLIM5) protein acts as a scaffold to tether various functional proteins at subcellular sites via PDZ and three LIM domains. Splicing of the ENH primary transcript generates various products with different repertories of protein interaction modules. Three LIM-containing ENH predominates in neonatal cardiac tissue, whereas LIM-less ENHs are abundant in adult hearts, as well as skeletal muscles. Here we examine the timing of splicing transitions of ENH gene products during postnatal heart development and C2C12 myoblast differentiation. Real-time PCR analysis shows that LIM-containing ENH1 mRNA is gradually decreased during postnatal heart development, whereas transcripts with the short exon 5 appear in the late postnatal period and continues to increase until at least one month after birth. The splicing transition from LIM-containing ENH1 to LIM-less ENHs is also observed during the early period of C2C12 differentiation. This transition correlates with the emergence of ENH transcripts with the short exon 5, as well as the expression of myogenin mRNA. In contrast, the shift from the short exon 5 to the exon 7 occurs in the late differentiation period. The timing of this late event corresponds to the appearance of mRNA for the skeletal myosin heavy chain MYH4. Thus, coordinated and stepwise splicing transitions result in the production of specific ENH transcripts in mature striated muscles.

1. Introduction

PDLIM proteins constitute a family of anchoring proteins that contain a PDZ domain and one to several LIM domains [1]. PDZ and LIM domains are protein interaction modules with distinct characteristics. PDZ domains consist of 80–90 amino acid residues and in many cases bind to a C-terminal peptide motif of cytoskeletal and membrane proteins. On the other hand, LIM domains are composed of two zinc-finger motifs and mediate interaction with various signaling molecules and transcription factors. Thus, PDLIM proteins are considered to act as scaffolds to assemble cellular signal-controlling molecules at certain subcellular sites.

ENH, Enigma homologue, is a member of PDLIM family (PDLIM5) containing a PDZ domain at the N-terminal region and three LIM domains in the C-terminal portion [2]. The PDZ domain of ENH binds to alpha-actinin and actin [3,4], whereas the LIM domains interact with protein kinases, such as several PKCs and PKD1 [2,5], as well as the transcription factor Id2 [6] and the neuronal postsynaptic protein SPAR [7]. ENH has been shown to sequester Id2 in the cytosol to prevent its transcriptional activity and neural differentiation [6], whereas ENH appears to alter the spine morphology of neuronal dendrites [7]. We have also shown that regulation of L-type Ca^{2+} channel by PKD1 requires scaffolding of these proteins by ENH [5]. Thus, ENH controls diverse cellular functions in neurons and cardiac myocytes by interacting with various molecules.

Although the identified cellular functions are based on the presence of both PDZ and LIM domains, the ENH gene generates splicing isoforms that lack LIM domains. In particular, the splicing variants ENH3 and ENH4 are predominant in cardiac and skeletal muscles in adult animals [3,4,8]. These two variants, as well as ENH2, are generated by inclusion of the exon 11, resulting in the insertion of a termination codon before the C-terminal region containing three LIM domains. Our previous work also revealed the important role of ENH splicing in the development of cardiac hypertrophy [8]. Aortic banding-induced hypertrophied myocardium appears to contain more ENH1 with three LIM domains and less ENHs without LIM domains. Furthermore, overexpression of ENH1 in neonatal myocytes results in hypertrophy, whereas LIM-less ENH4 prevents myocyte hypertrophy induced by various extracellular stimuli. These findings indicate that the splicing transition of ENH is a key event

* Corresponding author at: Department of Bioengineering, Nagaoka University of Technology, 1603-1 Kamitomioka, Nagaoka, Niigata 940-2188, Japan. Fax: +81 258 47 9401.
E-mail address: maturana@vos.nagaokaut.ac.jp (A.D. Maturana).

0006-291X/$ - see front matter © 2012 Elsevier Inc. All rights reserved.
http://dx.doi.org/10.1016/j.bbrc.2012.03.142

in the development of cardiac hypertrophy. They also suggest a unique role of LIM-less ENHs in striated muscles.

We wish to elucidate molecular mechanisms underlying the splicing transitions of ENH. In this report, we examine splicing transitions of ENH during postnatal heart development and C2C12 myoblast differentiation *in vitro*. We show here that the generation of cardiac and skeletal muscle-selective ENH variants is controlled by splicing events that occur at distinct differentiation periods.

2. Materials and methods

2.1. Animals

Care and handling of animals were in accordance with institutional guidelines and were approved by the Animal Care and Use Committees of the Tokyo Institute of Technology and the Nagaoka University of Technology. Experiments were performed using Sprague Dawley rats. Adult tissues were obtained from 250 to 300-g male animals (12–15 weeks old), whereas postnatally-developing heart tissues were from animals in both sexes at various postnatal days from multiple littermates. Ventricles were obtained by eliminating the top part of the isolated hearts containing atrial and aortic tissues. The obtained tissues were washed with ice-cold phosphate-buffered saline, cut into small pieces and frozen on dryice.

2.2. Cell culture

Mouse skeletal C2C12 cells were obtained from RIKEN BRC Cell Bank (Ibaraki, Japan). Cells were maintained in Dulbecco's Modified Eagle Medium supplemented with 10% fetal bovine serum (Gibco, Auckland, NZ), 50 U/ml penicillin and 50 μg/ml streptomycin (Nacalai Tesque, Kyoto, Japan) under 5% CO_2 atmosphere at 37 °C. For differentiation, cells were passed on plastic dishes at ~50% and cultured until semi-confluence (~90%). Culture medium was then switched to the low serum medium containing 2% fetal bovine serum. The medium was changed once every three days during the entire experimental period.

2.3. Real-time PCR analysis

Total RNA was isolated from heart tissues and C2C12 cells using a commercial reagent (TRIzol reagent, Invitrogen). The first-strand cDNA was synthesized using a commercial kit (ReverTra Ace qPCR RT Kit, Toyobo, Tokyo, Japan) according to the manufacturer's instructions. Real-time PCR was done with synthesized cDNA (50 ng of RNA content), 250 nM primers, and commercial master mix (KAPA SYBR FAST qPCR Kit, Kapa Biosystems, Woburn, MA) in a final volume of 25 μl. The PCR reaction was carried out in 96-well plates using Stratagene Mx3000P (Agilent Technologies, Santa Clara, CA).

Primers were designed to detect individual ENH variants (see Fig. 1A and B), as previously published [8], except that detection of mouse ENH3 mRNA was done with the reverse primer that corresponded to the exon 8: 5′-GTGGGCGTTTGGGTGGAATTTTC-3′. We used clones (T-Vector pMD20, Takara, Otsu, Shiga, Japan) each containing individual target PCR products as standards for quantitation. We also used skeletal marker genes for analysis: skeletal myosin heavy chain (GenBank Accession#: NM_010855), 5′-CTGACCGAGCA GATTGCTGAG-3′ (Nucleotide 4636-4656) 5′-ATCCTCAGAGCAT-CATTCCTGCTG-3′ (Nucleotide 4943-4920); and myogenin (GenBank Accession#:NM_031189), 5′-TCACATAAGGCTAACAC CCAGC-3′ (Nucleotide 876-896), and 5′-GCACTCATGTCTCTCAAACG GT-3′ (Nucleotide 1090-1069).

2.4. Semi-quantitative PCR analysis

We used semi-quantitative measurement of PCR products to estimate exon usages in the region encompassing the exon 5–8. For this analysis, standard PCR was performed in a final volume of 25 μl containing synthesized cDNA (50 ng of RNA content), 400 nM primers and commercial master mix (EmeraldAmp MAX PCR Master Mix, Takara, Otsu, Shiga, Japan). Primers corresponded to a part of the exon 3 and 9. The 5′ primer sequence was 5′-GAAGCCCAGAACAAGATTAAGGC-3′ for both species, whereas the 3′ primers were the ones used to detect ENH4 (see Fig. 1A and B). PCR conditions were 95 °C for 5 s, 64 °C for 10 s, and 72 °C for 60 s for 25–30 cycles with the final extension at 72 °C for 4 min. The PCR products were resolved by electrophoresis on a 3.5% agarose gel and stained with 0.5 μg/ml ethidium bromide. We cloned several PCR products obtained by this process into T vector (T-Vector pMD20) and sequenced.

For semi-quantitation of the PCR products, images were captured, and band intensity was measured using a charged coupled device-based camera system (Ultra-Violet Products, Upland, CA). Briefly, background was eliminated using the joint valley procedure, and the integral optical density was determined by the perpendicular drop method.

2.5. Data analysis

The mRNA levels were determined with a cDNA standard with or without normalization using cyclophilin mRNA as a control. We found that cyclophilin mRNA level substantially reduced during differentiation of C2C12 cells. Therefore, we used the data without normalization for C2C12 cells, whereas normalization with cyclophilin mRNA was used for the animal samples unless otherwise stated. Statistical analysis was performed by one-way *ANOVA*, followed the layered *Bonferroni*'s test. Data are presented as the mean ± SEM. $^{*}p < 0.05$, $^{**}p < 0.001$ and $^{***}p < 0.0001$ compared to day 1 for postnatal heart development and day 0 for C2C12 differentiation.

3. Results

3.1. Expression of ENH splicing variants during postnatal heart development

Previous studies have shown that LIM-less ENHs are abundant in the heart and skeletal muscle of adult rodents [3,4,8]. We first tested whether different adult organs might selectively express individual ENH splicing products. We designed primers that target the regions each unique for a subset of splicing variants (Fig. 1A and B). Specifically, ENH1 primers were targeted to the LIM region, whereas ENH3 and ENH4 primers detected transcripts containing the exons 5–8 and 6, respectively. Real-time PCR analysis revealed that different ENH splicing variants are predominant in adult rat organs. In the ventricle of the heart, ENH3 mRNA was more than 10 and 100 times abundant than ENH1 and ENH4 transcripts, respectively (ENH variant/cyclophilin mRNA ratio (%): ENH1 = 0.18 ± 0.09, ENH3 = 1.98 ± 0.55, ENH4 = 0.016 ± 0.007, $n = 3$). In contrast, ENH4 mRNA is the most abundant in the skeletal muscle (ENH1 = 0.07 ± 0.04, ENH3 = 0.13 ± 0.10, ENH4 = 8.3 ± 2.1, $n = 3$), whereas only ENH1 transcript was significant in the brain (ENH1 = 0.15 ± 0.010, ENH3 = 0.001, ENH4 < 0.001, $n = 3$). Thus, although the absolute levels of ENH variants largely differ among adult rat organs, fully developed organs selectively express individual ENH splicing variants.

Our previous study indicated that the levels of ENH splicing variants markedly differ between newborn and adult heart tissues [8]. To determine the timing of this splicing transition, we measured

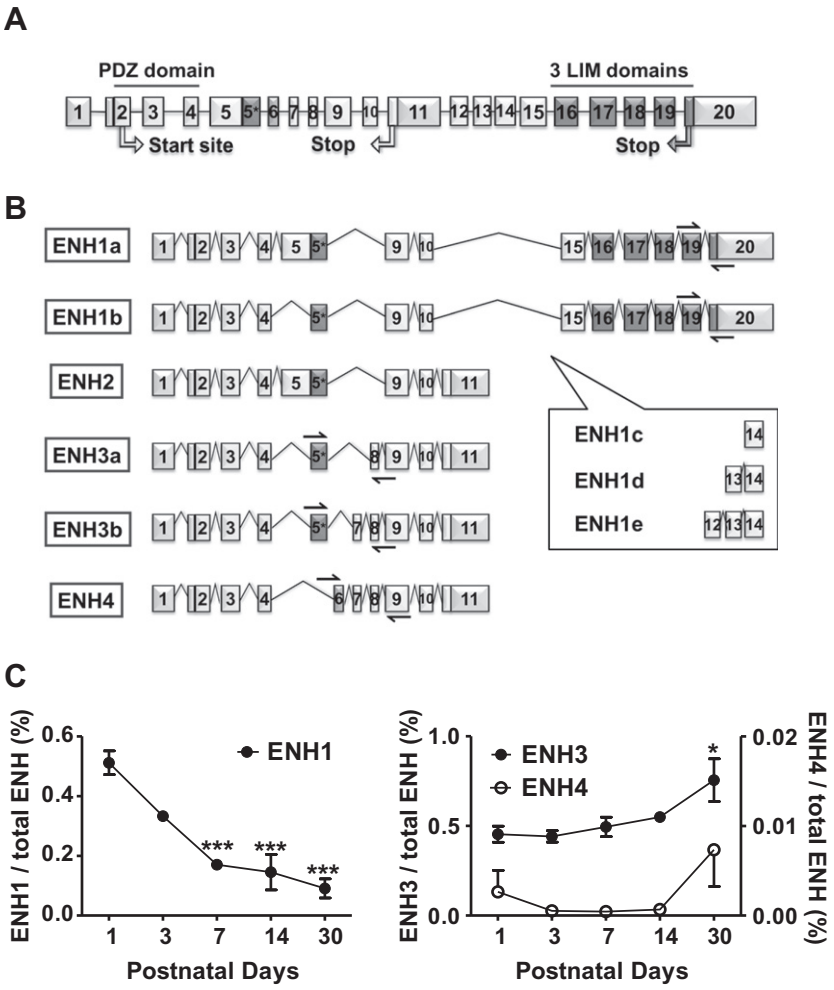

Fig. 1. Expression of ENH splicing variants in postnatal heart development. (A) A diagram is based on the reported genomic organization of the mouse ENH gene [10]. The rat genome possesses primarily the same organization, except that the first non-coding exon is present [8]. We use the exon numbers based on the reported mouse genome in this article. (B) Diagrams indicate the known splicing variants. Arrows indicate the positions of primer used in this study. (C) Real-time PCR were performed with primer sets that were designed to detect transcripts containing the exons 17–18 (ENH1), the exons 5 and 8 (ENH3), or the exon 6 (ENH4). ENH1-3 mRNA levels are presented as the ratio to total ENH mRNA level ($n = 3$).

splicing variant and total ENH mRNAs during postnatal development of rat hearts (Fig. 1C). Total ENH mRNA level determined using a primer set for the PDZ region showed no significant change during the entire postnatal period. ENH1 mRNA level was gradually reduced during postnatal heart development, whereas expression of ENH3 transcript was significant at birth and doubled in the late postnatal days. Although the absolute level of ENH4 mRNA was more than 100 times lower than that of ENH3 transcript, ENH4 mRNA level was below the detection limitation at the birth and in the early postnatal days, but became significant at the late postnatal days. These results indicate that the splicing transitions from LIM-containing ENH1 to LIM-less ENHs occur during postnatal heart development. Yet, the observed reduction in ENH1 mRNA is not fully accounted for by the rise in the expression of ENH3 and ENH4 transcripts.

Recent study indicated that ENH splicing is more complex than initially anticipated [10], generating diverse splicing variants in the adult mouse heart. This complexity is originated from splicing events in the two regions: the region encompassing the exons 5–8 and the portion in front of the exon 15 (see Fig. 1A and B). Any exon usages at the latter region should result in LIM-containing ENH variants that were detected with our ENH1 primers. In contrast, our ENH3 primers might miss some exon combinations in the former region. Thus, we set out PCR analysis to test for exon shuffling in the exons 5–8 region using the primers that correspond to the outside of this portion (Fig. 2A). PCR with these primers should detect various exon combinations as bands with distinct sizes. We found at least four products with different sizes in the ventricle of adult hearts (Fig. 2B). Cloning and sequencing of these products revealed that the largest band corresponded to the variants with the long exon 5+ the exon 7+ the exon 8, whereas the three smaller bands contained the short exon 5 with or without the other two exons (Fig. 2A). Thus, the adult cardiac tissue contains multiple transcripts with various exon combinations in the exons 5–8 portion.

During postnatal heart development, the ratio of these bands markedly changed (Fig. 2C and D). The products with the long exon 5 (565-bp band) and the short exon 5+ the exon 7+ the exon 8 (271-bp band) dramatically increased in the late postnatal days. Moreover, the transcripts containing the short exon 5 and exon 8 were the major forms in the early developmental days, whereas the ones without the exon 7 or 8 remained relatively constant during the postnatal period. Thus, ENH transcripts undergo complex splicing transitions during postnatal heart development.

3.2. Splicing transitions of ENH during differentiation of C2C12 myoblasts

We also tested if the splicing transitions of ENH might take place in the development of skeletal muscle using C2C12 myoblast

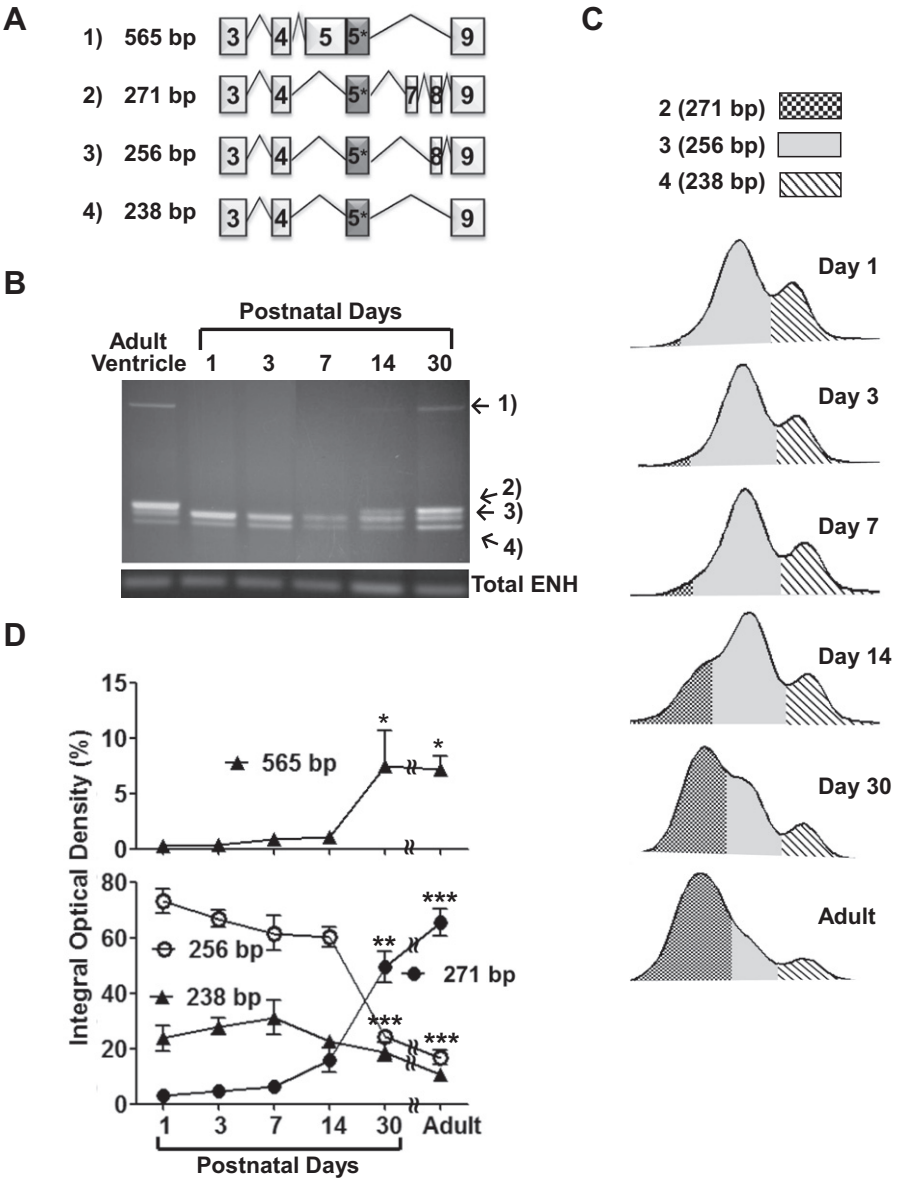

Fig. 2. Splicing patterns in the region encompassing the exons 5–8 during postnatal heart development. (A) PCR was performed with forward and reverse primers corresponding to the sequence in the exons 3 and 9, respectively. Major bands obtained by PCRs were cloned and sequenced. Diagrams represent exon combinations of the major bands obtained by the PCR analysis and confirmed by sequencing. (B) PCR results are shown with arrows indicating the positions of major bands. (C) Optical density for each band was estimated as described in Section 2. Graphs indicate optical intensity along each lane for the region encompassing the bands 2–4). Different shadowing areas represent the integral optical density for the bands 2–4). (D) Total and individual band intensities were calculated using the data in (C). Integral optical density represents the ratio to the sum of integral optical density as percentages ($n = 3$).

cells. We first measured mRNA levels for ENH1, ENH3 and ENH4, as well as total ENH, using primers that were designed similarly to the measurement with the heart samples. Reducing serum concentration induced the formation of myotube-like morphology and expression of the skeletal muscle marker genes (Fig. 3A and B). We found that total ENH mRNA level remained constant during the entire differentiation period. Similarly to postnatally-developing hearts, ENH transcripts exhibited the shift from LIM-containing ENH1 to LIM-less ENHs during C2C12 differentiation (Fig. 3C). Moreover, the time course changes in the two LIM-less ENH transcripts seemed to differ. ENH3 mRNA reached the highest level at days 3 and 5. This time course change was similar to the appearance of myogenin mRNA, an early-onset gene during C2C12 differentiation [9]. In contrast, the expression of ENH4 transcripts slowly rose at day 3 and continued to increase until the end of the experimental period at day 7. A similar late-onset change was seen with mRNA for the skeletal myosin heavy chain (MYH4), a late-onset gene during C2C12 differentiation. Thus, the expression of ENH variants during C2C12 differentiation may involve coordinated and stepwise splicing transitions.

Since we found multiple and complex uses of the exons 5–8 in the heart, the same strategy was used to examine for exon combinations in C2C12 cells (Fig. 4A). We detected one very strong and several minor bands in undifferentiated C2C12 cells (Fig. 4B). Sequencing of some of these products revealed that the strong band at ~570 bp corresponded to the long exon 6 without any additional exons, whereas the minor band at ~240 bp was matched to the short exon 6 (Fig. 4A). During differentiation, the ~570-bp band gradually reduced. Instead, the bands at ~200 and ~260 bp appeared. The intensity of the larger band at ~260 bp peaked at days 3–5 during differentiation, whereas that of the smaller band at ~200 bp continued to increase until the end of

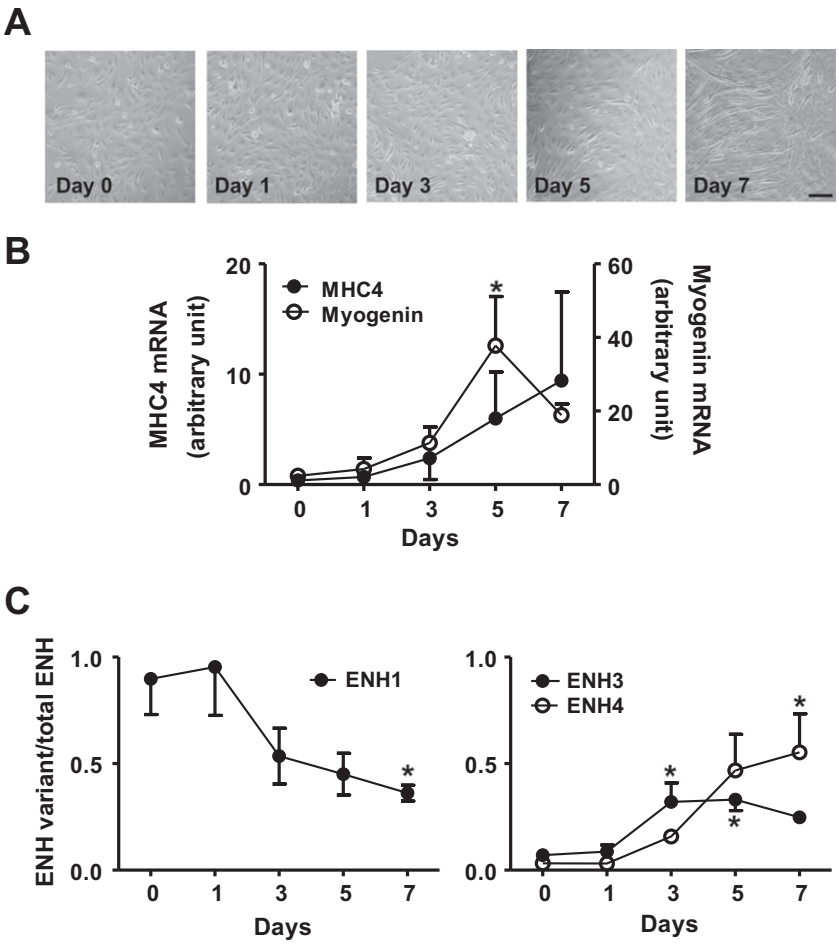

Fig. 3. Expression of ENH splicing variants during differentiation of C2C12 cells. (A) Pictures show bright field images of C2C12 cells upon reduction in serum concentration from 10% to 2%. Note that myotube-like structures become prominent in later days. A bar indicates the scale of 200 μm. (B) Graphs show the levels of myogenin and myh4 mRNAs during differentiation. Point and error bars indicate the mean ± SEM ($n = 3$). Note that the time course changes differ between the two marker mRNAs. (C) ENH variant mRNAs were measured by real-time PCR analysis, as described in the legend for Fig. 1 ($n = 3$).

experimental period (Fig. 4C). We also found that only the smaller band at ~200 bp was significant in the adult skeletal muscle tissue (Fig. 4B, left lane). These time course changes were reminiscent of those observed for ENH3 and ENH4 transcripts, respectively. Sequencing of these bands confirmed this prediction: the larger band at ~260 bp corresponded to transcripts with the short exon 5+ the exon 8, whereas the smaller band at ~200 bp included the exons 6, 7, and 8. These results suggest that ENH transcripts undergo the two-step transitions during C2C12 differentiation: the first shift from the long exon 5 to the short exon 5, and the second from the short exon 5 to the exon 6. Taken together, our data imply that differentiation of myoblastic cells are associated with the stepwise splicing transitions of ENH, leading to the skeletal muscle-selective expression of ENH4 isoform containing the exons, 6, 7, and 8.

4. Discussion

RNA splicing is a ubiquitous mechanism to generate protein isoforms with functional diversity. This study examined splicing transitions of the single RNA molecule encoding the anchoring protein ENH. Our data indicate that different adult rat organs selectively express distinct ENH variants. Cardiac muscle contains LIM-less ENHs with various combinations of the exons 5, 7 and 8, whereas adult skeletal muscle expresses LIM-less ENH4 containing the exons 6, 7, and 8. Although we did not analyze transcripts in detail, ENH1s with three LIM domains are predominant in the brain. The identified LIM-less ENH variants should exhibit substantially different functions in striated muscles, compared to three LIM-containing ENH1 whose functions are assigned based on its ability to assemble signaling molecules by their LIM domains [6–8]. Selective use of the exons 6–8 in skeletal muscle may also fulfill special requirement in this striated muscle.

In the developing heart, splicing transitions occur in a large number of transcripts [11,12] and their temporal changes can be divided into three patterns [12]. Many transitions take place primarily in prenatal or postnatal period, whereas others occur in both two phases. Although this study examined splicing changes only in the postnatal period, multiple transitions of ENH transcripts appear to take place in this period. Expression levels of several RNA-binding proteins, such as FOX-1 and CUGBPs, are markedly changed during the late postnatal period and influence splicing transitions of various transcripts [12]. Therefore, these factors may also control the observed ENH splicing transitions. Our results further support the possibility that the splicing transitions of ENH transcripts occur in temporally-distinct phases during postnatal heart development. The shift from LIM-containing ENHs to LIM-less ENHs occurred in the early postnatal days with a marked decline in the first 7 days after birth. This shift reflects the insertion of the exon 11. In contrast, the appearance of the long exon 5 and the inclusion of the exon 7 became apparent only in the late postnatal days 14 and 30. Thus, the splicing transitions of ENH

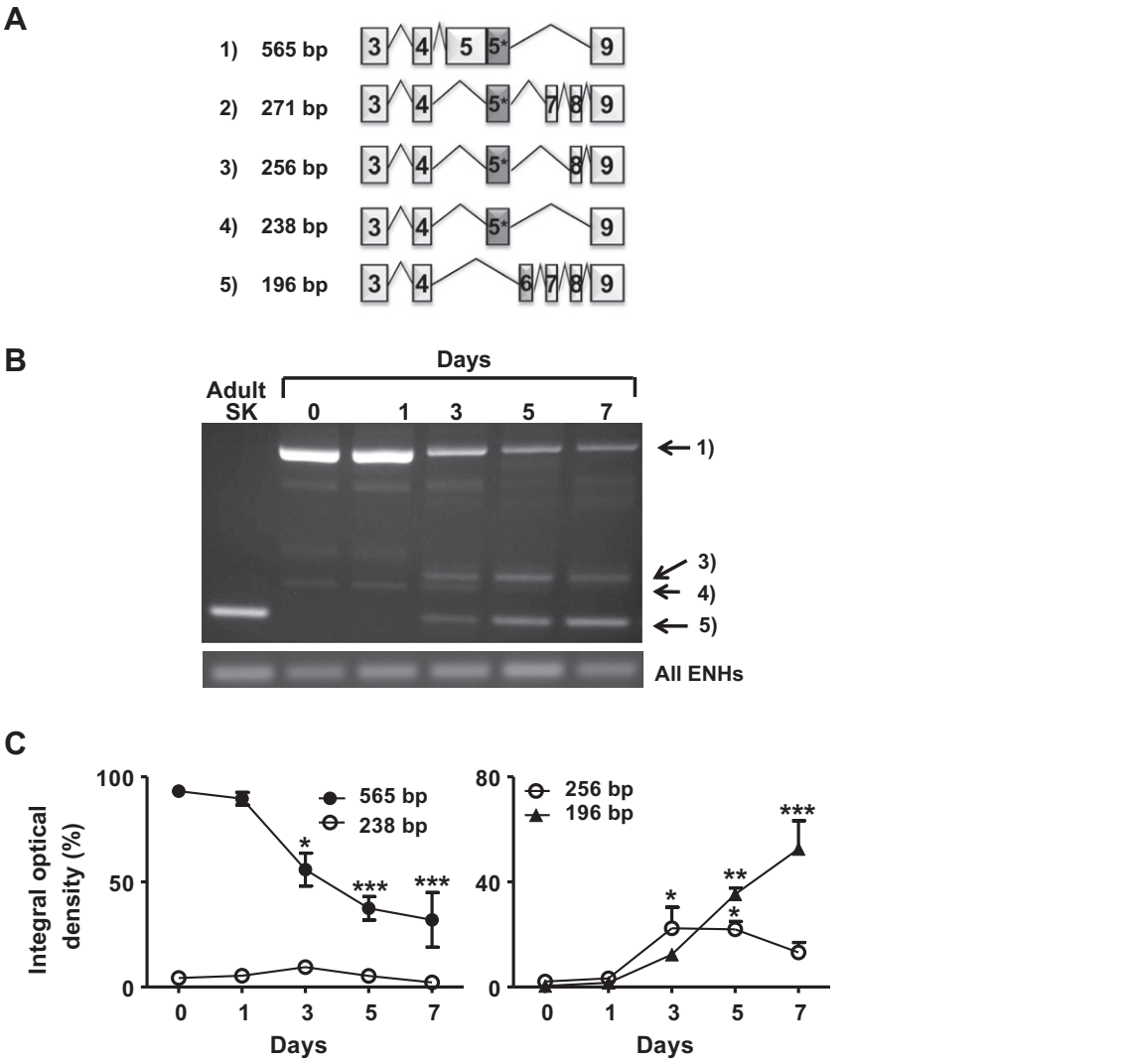

Fig. 4. Splicing patterns in the region encompassing the exon 6–9 during differentiation of C2C12 cells. (A) PCR was performed and major products were identified, as described in the legend for Fig. 3. The major products obtained are shown as diagrams. (B) PCR data are shown with arrows indicating the positions of the identified bands in (A). (C) Band intensities were semi-quantitatively estimated similarly to Fig. 3. Graphs show percentages of optical density (each band/total, $n = 3$).

transcripts may take place in a coordinated and stepwise fashion in developing hearts during the postnatal period. Mammalian hearts exhibit a large volume increase during the postnatal period. The volume increase of murine hearts in the first 7 days after birth is due to hyperplasia without cytokinesis (binucleation), whereas hypertrophy is largely responsible for the increased mass afterward [13]. We speculate that LIM-containing ENHs may be required for hyperplasia, whereas LIM-less ENHs with the long exon 5 or the exon 7 may possess functional/structural roles in mature cardiac muscles.

The splicing transitions of ENH in differentiating C2C12 cells may also be classified into temporally-distinct phases. In particular, the shift from the long exon 5 to the short exon 5 seems a hallmark of the early event, whereas the switch from the short exon 5 to the skeletal muscle-selective exon 6 occurs in the late differentiation period. A microarray analysis during C2C12 differentiation has categorized genes into several expression patterns [9]. A previous large-scale splicing analysis also shows distinct time-courses of splicing transitions during C2C12 differentiation [14]. These previous studies primarily identified the two distinct stages, early and late phases of differentiation. The observed ENH splicing transition from the long exon 5 to the short one is likely categorized as an event in the early phase, whereas the switch from the short exon 5 to the exon 6 seems to represent a change in the late phase. We should note that the use of the exon 6 is correlated with the insertion of the exons 7 and 8. Indeed, we detected no transcripts containing the exons 6 without the exon 7 or 8 in differentiating C2C12 cells and adult skeletal muscle. Thus, the late splicing transition of ENH transcript may include simultaneous insertion of these three exons. Since these splicing transitions are prominent in skeletal muscle-like cells and native tissue, skeletal muscle-specific factors may be responsible for these late stage events in C2C12 differentiation.

The reduction in LIM-containing ENH1s is commonly seen during postnatal heart development and C2C12 differentiation. Yet, we found substantial differences in the use of the exons 5–8 between the two developmental/differentiation processes. An obvious difference is in the use of the internal junction in the exon 5. Transcripts with the long exon 5 were significant only in the hearts at the late postnatal days and adulthood. In contrast, they were predominant forms in undifferentiated C2C12 cells, but were markedly reduced during differentiation. Thus, the two types of striated muscles might use different controlling mechanisms for this splicing transition. In addition, the splicing selection of the

exons 5–8 markedly differs between cardiac and skeletal muscles in adult animals. The adult skeletal muscle almost exclusively uses the combination of the exons 6, 7, and 8, whereas the ventricular tissue contains multiple exon combinations. The observed complexity in the ventricle might arise from various cell types present in the tissue. For example, the ventricule contains a large number of cardiac fibroblasts. Many cell lines including fibroblastic cells are known to express ENH mRNAs [3]. Therefore, it is possible that the detected ENH transcripts may, in part, represent the expression in cardiac fibroblasts and other residential cells in the ventricular tissue. However, we observed transcripts with multiple combinations of the exons 5–8 in cultured neonatal myocytes largely devoid of non-myocytes (data not shown). Hence, the mechanisms controlling splicing of the exons 5–8 may significantly differ between cardiac and skeletal muscles.

Taken together, we have analyzed splicing transitions of the anchoring protein ENH during striated muscle development. The splicing transitions of ENH transcripts between developing hearts and differentiating C2C12 cells exhibit similarities and differences. The incorporation of the exon 11 is commonly increased during striated muscle development, whereas the two maturing/differentiation processes largely differ in the use of the exons 5–8. Our data also support that the splicing events are coordinated and stepwise during striated muscle development. Specifically, the splicing transitions of ENHs may be divided into two temporally-distinct phases in postnatally-developing hearts and differentiating C2C12 cells. Hence, single gene transcripts may undergo multiple splicing transitions in cell type- and developmental stage-specific manners.

References

[1] A.J. Te Velthuis, T. Isogai, L. Gerrits, C.P. Bagowski, Insights into the molecular evolution of the PDZ/LIM family and identification of a novel conserved protein motif, PLoS ONE 2 (2007) e16047.

[2] S. Kuroda, C. Tokunaga, Y. Kiyohara, O. Higuchi, H. Konishi, K. Mizuno, G.N. Gill, U. Kikkawa, Protein–protein interaction of zinc finger LIM domains with protein kinase C, J. Biol. Chem. 271 (1996) 31029–31032.

[3] N. Nakagawa, M. Hoshijima, M. Oyasu, N. Saito, K. Tanizawa, S. Kuroda, ENH, containing PDZ and LIM domains, heart/skeletal muscle-specific protein, associates with cytoskeletal proteins through the PDZ domain, Biochem. Biophys. Res. Commun. 272 (2000) 505–512.

[4] N. Niederlander, N.A. Fayein, C. Auffray, P. Pomies, Characterization of a new human isoform of the enigma homolog family specifically expressed in skeletal muscle, Biochem. Biophys. Res. Commun. 325 (2004) 1304–1311.

[5] A.D. Maturana, S. Walchli, M. Iwata, S. Ryser, J. Van Lint, M. Hoshijima, W. Schlegel, Y. Ikeda, K. Tanizawa, S. Kuroda, Enigma homolog 1 scaffolds protein kinase D1 to regulate the activity of the cardiac L-type voltage-gated calcium channel, Cardiovasc. Res. 78 (2008) 458–465.

[6] A. Lasorella, A. Iavarone, The protein ENH is a cytoplasmic sequestration factor for Id2 in normal and tumor cells from the nervous system, Proc. Natl. Acad. Sci. USA 103 (2006) 4976–4981.

[7] S. Herrick, D.M. Evers, J.Y. Lee, N. Udagawa, D.T. Pak, Postsynaptic PDLIM5/Enigma Homolog binds SPAR and causes dendritic spine shrinkage, Mol. Cell Neurosci. 43 (2010) 188–200.

[8] T. Yamazaki, S. Walchli, T. Fujita, S. Ryser, M. Hoshijima, W. Schlegel, S. Kuroda, A.D. Maturana, Splice variants of enigma homolog, differentially expressed during heart development, promote or prevent hypertrophy, Cardiovasc. Res. 86 (2010) 374–382.

[9] K.K. Tomczak, V.D. Marinescu, M.F. Ramoni, D. Sanoudou, F. Montanaro, M. Han, L.M. Kunkel, I.S. Kohane, A.H. Beggs, Expression profiling and identification of novel genes involved in myogenic differentiation, FASEB J. 18 (2004) 403–405.

[10] H. Cheng, K. Kimura, A.K. Peter, L. Cui, K. Ouyang, T. Shen, Y. Liu, Y. Gu, N.D. Dalton, S.M. Evans, K.U. Knowlton, K.L. Peterson, J. Chen, Loss of enigma homolog protein results in dilated cardiomyopathy, Circ. Res. 107 (2010) 348–356.

[11] H.W. Chen, S.L. Yu, W.J. Chen, P.C. Yang, C.T. Chien, H.Y. Chou, H.N. Li, K. Peck, C.H. Huang, F.Y. Lin, J.J. Chen, Y.T. Lee, Dynamic changes of gene expression profiles during postnatal development of the heart in mice, Heart 90 (2004) 927–934.

[12] A. Kalsotra, X. Xiao, A.J. Ward, J.C. Castle, J.M. Johnson, C.B. Burge, T.A. Cooper, A postnatal switch of CELF and MBNL proteins reprograms alternative splicing in the developing heart, Proc. Natl. Acad. Sci. USA 105 (2008) 20333–20338.

[13] F. Li, X. Wang, J.M. Capasso, A.M. Gerdes, Rapid transition of cardiac myocytes from hyperplasia to hypertrophy during postnatal development, J. Mol. Cell. Cardiol. 28 (1996) 1737–1746.

[14] C.S. Bland, E.T. Wang, A. Vu, M.P. David, J.S. Castle, J.M. Johnson, C.B. Burge, T.A. Cooper, Global regulation of alternative splicing during myogenic differentiation, Nucleic Acids Res. 38 (2010) 7651–7664.